Published in final edited form as:

Wiley Interdiscip Rev RNA. 2016 September ; 7(5): 683–701. doi:10.1002/wrna.1358.

Lights, Camera, Action! Capturing the Spliceosome and pre-mRNA Splicing with Single Molecule Fluorescence Microscopy

Alexander C. DeHaven[1,2,†], **Ian S. Norden**[1,2,†], and **Aaron A. Hoskins**[2,*]

[1]Integrated Program in Biochemistry, U. Wisconsin-Madison, Madison, WI 53706

[2]Department of Biochemistry, U. Wisconsin-Madison, Madison, WI 53706

Abstract

The process of removing intronic sequences from a precursor to messenger RNA (pre-mRNA) to yield a mature mRNA transcript via splicing is an integral step in eukaryotic gene expression. Splicing is carried out by a cellular nanomachine called the spliceosome that is composed of RNA components and dozens of proteins. Despite decades of study, many fundamentals of spliceosome function have remained elusive. Recent developments in single molecule fluorescence microscopy have afforded new tools to better probe the spliceosome and the complex, dynamic process of splicing by direct observation of single molecules. These cutting-edge technologies enable investigators to monitor the dynamics of specific splicing components, whole spliceosomes, and even co-transcriptional splicing within living cells.

Graphical Abstract

[*]Correspondence to: ahoskins@wisc.edu.
[†]These authors contributed equally.

Cross-References

DOI	Article title
WRNA.83	Techniques for following the movement of single RNAs in living cells
WRNA.1115	RNA biology in a test tube—an overview of in vitro systems/assays
WRNA.86	Pre-mRNA splicing during transcription in the mammalian system

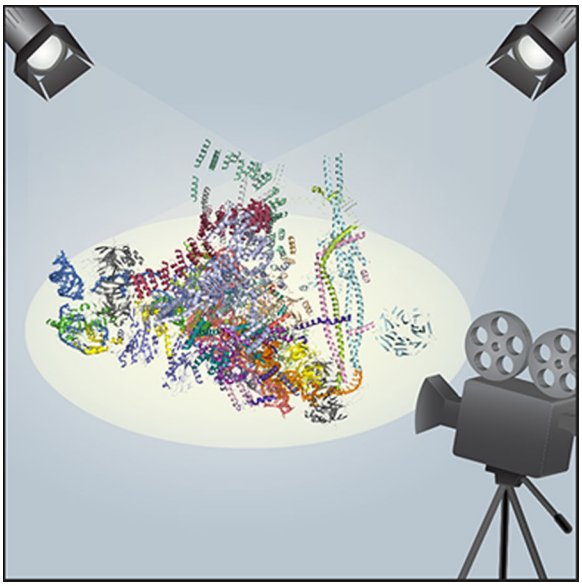

Keywords

Single Molecule; Fluorescence; FRET; CoSMoS; Colocalization; dcFCCS; Splicing; pre-mRNA; Spliceosome; snRNP; snRNA; RNA; Dynamics

The spliceosome is undoubtedly one of the most complicated machines inside the cell. Containing a core of ~100 proteins and 5 small nuclear RNAs (snRNAs),[1] the spliceosome assembles on introns to catalyze concomitant intron excision and exon ligation via two sequential transesterification reactions. The full cohort of splicing factors in humans includes hundreds of additional proteins,[2] and the spliceosome plays a central role in establishing the diversity of the cellular transcriptome through alternative splicing.[3] Unraveling spliceosome biochemistry given the machine's complexity, malleability, and sheer number of splicing factors is a formidable challenge. Practically speaking, many of the challenges facing spliceosome biochemists can be boiled down to the observation that splicing reactions are frequently quite messy: they often contain a relatively low concentration of spliceosomes of various compositions all carrying out different steps in splicing at different times.

Single molecule methods are adept at tackling unsynchronized and heterogeneous reactions and by definition are well suited for studying dilute samples. Using these approaches, molecules can be grouped according to similar patterns of behavior during data analysis after the experiment has been completed.[4] For the spliceosome, this means that dead-end complexes can easily be distinguished from those "on-path" towards splicing and that spliceosomes exhibiting different types of heterogeneity (conformational, compositional, or even those assembled by different pathways) can be identified and analyzed separately. Many single molecule methods are now routinely being used by biochemists including fluorescence, force, and electron microscopic (EM) based approaches. In this review we focus on recent applications of single molecule fluorescence microscopy to study various aspects of spliceosome biochemistry and splicing both in the test tube and in cells.

Molecules and Methods

The fields of both splicing and single molecule biochemistry are filled with a number of specialized terms and concepts. In this section, short overviews of the spliceosome and single molecule fluorescence-based methods will be given to lay the foundation for the more detailed experimental approaches and insights into splicing that follow.

The pre-mRNA Splicing Machinery

The spliceosome has been subject to a wide-range of studies over the past few decades, and we currently know a tremendous amount about spliceosome composition and the fundamentals of splicing biochemistry (see Wahl, Will, and Lührmann[5] and Papasaikas and Valcárcel[6] for recent reviews). The largest subunits of the spliceosome are the small nuclear ribonucleoproteins (snRNPs) that each contain a snRNA and subset of spliceosomal proteins. Spliceosomes are assembled from snRNPs onto intron-containing pre-mRNAs at locations identified by specific intronic sequences including the 5' and 3' splice sites (SS) and the branchsite (BS). An adenosine within the BS provides the nucleophile for the first chemical step in splicing, 5' SS cleavage and lariat formation. The liberated 5' exon in turn provides a 3' OH group that serves as the nucleophile for the second chemical step in splicing (exon ligation) that produces the mRNA and lariat-intron products.

Spliceosomes undergo distinct stages of assembly, activation (during which the active site is formed), catalysis, disassembly/product release, and recycling of the splicing factors (Figure 1). Spliceosomes are single turnover enzymes, and different spliceosomes are responsible for removing different introns in a multi-intronic transcript. In addition to the snRNPs, a number of other protein splicing factors participate in splicing.[5] Some of these factors are required for spliceosome function, while others can regulate the splicing of alternatively spliced exons.[3] Splicing requires ATP hydrolysis, and a number of spliceosomal proteins are DExD/H-box RNA-dependent ATPases that facilitate transitions between one spliceosome complex and another as well as enforce splicing fidelity.[5,7,8] To date, the major targets of single molecule studies of splicing have been understanding the pathways *S. cerevisiae* (yeast) spliceosomes take between different reaction stages, the dynamic conformational landscape of the spliceosomal snRNAs and pre-mRNA substrate during splicing, and the coupling between conformational changes and the presence or absence of various splicing factors. Single molecule studies in cells, on the other hand, have often focused on where and when splicing occurs in the nucleus as well as coupling between splicing and other steps in RNA processing.

Single Molecule Fluorescence Microscopy Techniques

Single molecule fluorescence experiments *in vitro* can be broadly separated into two categories: those in which biomolecules are immobilized on a surface and those in which the molecules are untethered and diffusing.[9] Both types of experiments can yield information on molecular composition and conformation, usually by studying the colocalization of multiple fluorophores with different fluorescence excitation and emission wavelengths or by studying how these fluorophores interact with one another through Förster resonance energy transfer (FRET). Immobilization methods are well suited for studying individual molecules for long

periods of time, while tether-independent methods provide brief snapshots of molecules as they freely diffuse through the observation volume.

Microscopes used for studying single molecules by light microscopy range from commercial, turn-key systems to custom set-ups constructed to fulfill particular experimental objectives. Details of the construction and properties of these microscopes are beyond the scope of this review; however, many recent publications have appeared on this topic.[10–14] Instead we will focus on general features of experiments detecting either tethered or untethered molecules.

In the most common types of experiments involving immobilization (Figure 2a), a fluorescent biomolecule is tethered to a glass or quartz surface via a direct covalent bond or non-covalently through interactions with antibodies or by using biotin/streptavidin. The immobilized molecules are then viewed with a microscope usually with a laser excitation source, a high numerical aperture (NA) objective, and either a cooled electron multiplying-charge coupled device (EM-CCD) or complementary metal-oxide-semiconductor (CMOS) camera. Often the molecules are excited via total internal reflectance (TIR) to further reduce background and increase signal-to-noise. In order to observe freely diffusing molecules, dilute solutions of fluorescent molecules (typically < 10 nM) are routinely imaged using a microscope with use of a confocal (pinhole) aperture in the emission pathway to increase signal-to-noise and remove out-of-focus fluorescence emission. As the biomolecules diffuse through a confocal collection volume, they will become excited and emit photons (Figure 2b). These photons can then be collected using very sensitive and fast avalanche photodiode detectors (APDs). While microscopes relying on confocal apertures are routinely employed, other strategies have recently been developed to permit observation of untethered molecules.[15–17]

Single Molecule FRET—In a single molecule FRET (smFRET) experiment, at least two fluorophores are used as a FRET pair—meaning that the emission spectrum of the donor fluorophore (*e.g.*, Cy3) overlaps with the excitation spectrum of the acceptor fluorophore (*e.g.*, Cy5). When the fluorophores are proximal, a high FRET signal is observed and this signal decreases the further apart the fluorophores become.[9,18] While this information can be used to calculate distances between the fluorophores,[19] in practice this technique is more often used for detecting and studying the dynamic transitions between two or more conformational states. Distance calculations can be difficult since factors such as the fluorophore orientation or stacking can complicate interpretation of the FRET signal.[20–23] In the simple case of a single biomolecule containing two FRET fluorophores and transitioning between two conformations with two different FRET values (Figure 2a, top), anti-correlated changes in FRET donor and acceptor fluorescence can be observed. These values are then often used to calculate a FRET efficiency (E_{FRET}), where $E_{FRET} = I_D/(I_A+I_D)$ and I_D and I_A represent the intensities of FRET donor (I_D) and acceptor (I_A) obtained by integration of a spot of single molecule fluorescence. Plots of changes in E_{FRET} over time for many molecules can then be used to deduce not only the number of conformational states present in the system but also the pathways and kinetics by which these states interconvert. This is routinely carried out by combining histogram analysis of measured E_{FRET} values along with

fitting the number of states observed on individual E_{FRET} traces by hidden Markov modeling (HMM) or Bayesian analysis.[24–26]

Single Molecule Colocalization—Colocalization experiments are similar to smFRET experiments in that multiple fluorophores are used; however, the goal of these experiments is often to determine the composition of a complex or to study the kinetics of complex formation. In an example 2-color colocalization experiment, each fluorophore is directly excited with its own laser and individually monitored (Figure 2a, bottom).[11] When a fluorescent biomolecule associates with an immobilized substrate, it can be detected as a peak in fluorescence intensity. Molecules passing through the focal plane are often not observed directly and contribute to the overall diffuse background fluorescence. Whether or not a bound molecule is detected in turn depends on its binding time (dwell time or τ), the camera frame rate, and the excitation laser power (faster frame rates often require higher laser powers to detect a signal). In these experiments, the dwell times of each interaction as well as the times between each binding event can be collected and fit to kinetic models to determine off- and on-rates, respectively.[11,12,27] Colocalization methods are particularly adept for studying pathways of macromolecular complex assembly or disassembly[11] and can be combined with smFRET to yield further information.[28]

Single Molecule Fluorescence from Freely Diffusing Molecules—By only detecting emission from one fluorophore, experiments studying single molecules in solution can yield information about diffusive properties, which in turn can be used to derive information such as molecular shape, composition, or concentration.[9] In fluorescence correlation spectroscopy (FCS), data from many single molecule bursts of fluorescence are often analyzed using an autocorrelation function ($G(\tau)$, Figure 2b) to deduce biomolecular interactions or conformational changes.[9] When more than one fluorophore is used simultaneously, additional information about molecular composition and binding properties can be obtained by correlating single molecule fluorescence signals obtained from each fluorophore with one another (dual-color fluorescence cross-correlation spectroscopy, dcFCCS).[29] Fluorescence from freely diffusing molecules containing multiple fluorophores can also yield valuable information through fluorescence-aided molecular sorting (FAMS) and histogram analysis,[23] although this approach has not yet been applied to the spliceosome.

Single Molecule Fluorescence in Cells—Seeing a single fluorophore inside a living or fixed cell remains a considerable challenge. While many super-resolution methods rely on the switching of a single fluorophore “on” or “off”,[30] these methods have had their greatest impact in studies of cellular anatomy in which many individual fluorophores contribute to the overall image (*e.g.*, the actin cytoskeleton). To observe discrete molecules in a cell, several approaches have been recently developed.[31] In some cases, the experiments are greatly facilitated by appending very bright fluorophores (*e.g.*, the cyanine (Cy) dyes used routinely for smFRET *in vitro*) to biomolecules of interest. These labeled biomolecules can first be prepared chemically or enzymatically and subsequently injected[32–34] or incorporated into cells.[35,36] Alternatively, chemical biology tools combined with sophisticated microscopy techniques can facilitate labeling of endogenous cellular proteins and single

molecule measurements.[37,38] The same types of confocal detection schemes used to study freely diffusing molecules in solution *in vitro* can also be used in cells to collect FCS data *in vivo*. In fact, FCS has already been used to analyze splicing factors as they move about within the nucleus.[39]

Bright fluorescence signals from a single RNA can be obtained by labeling transcripts with multiple fluorophores simultaneously.[40] In fixed cells, this is now routinely done using single molecule fluorescence *in situ* hybridization (smFISH; Figure 2c, bottom).[41–43] In smFISH, multiple oligonucleotides that are both complementary to a particular transcript of interest and carry a bright fluorophore are hybridized to cellular RNA targets in fixed, permeablized cells. Since a single transcript molecule will be labeled with dozens of fluorophores, it can now be easily observed and localized in the cell, often without requiring any sophisticated microscopy techniques. Recent advances in RNA barcoding and data analysis-algorithms have allowed many different transcripts, even hundreds, to be imaged simultaneously through fluorescent probe hybridization.[44,45]

In live cells, a similar strategy is often used. RNA transcripts can be genetically modified to incorporate multiple copies of a binding site for a RNA-binding protein, which is simultaneously expressed as a fusion to a fluorescent protein (FP).[40,46] An individual transcript molecule can then be observed above the cellular background fluorescence since it will contain multiple, often dozens, of bound FPs (Figure 2c, top). FP fusions to the phage coat proteins MS2 or PP7[47] and the λN peptide[48] have been well-characterized and used to observe single transcripts in live cells as they are being synthesized and processed.

Single Molecule Studies of Spliceosomes *in vitro*

In this section, single molecule studies of the splicing machinery carried out *in vitro* using purified components or in cell extracts are described. These experiments have shed new light on the dynamic properties of the spliceosome machinery as well as molecular and kinetic descriptions of pathways for spliceosome assembly and catalysis.

Model Systems for Studying RNA Dynamics during Splicing

Simplifying a complex machine to a well-defined model system can be a useful method for identifying specific functions or behaviors of one constituent out of many. Model proteins and RNAs have been used to study many components of the spliceosome including chemical reactions catalyzed by the snRNAs,[49–52] snRNA structure and function,[53–59] and the activities of various spliceosomal proteins and helicases.[60–65] In addition to these and other biochemical and structural experiments, single molecule analysis of models for various spliceosome components has played an important role in elucidating splicing dynamics. These insights are highlighted by recent results using models for the U2 snRNA and U2/U6 and U4/U6 di-snRNAs.

The stem II region of the U2 snRNA has been proposed to interconvert between two, mutually exclusive structures: stem IIa is required for recognition of the BS and pre-spliceosome formation while the stem IIc conformation is important but not essential for catalysis.[66,67] How these two conformations interconvert has been unclear with various

models proposed that include stabilization of stem IIc by the RNA-binding protein Cus2 and unwinding of stem IIc by the DEAD-box ATPase Prp5.[66–68] To study stem II conformational changes directly, Rodgers *et al.* designed a model yeast U2 snRNA that allowed for real time observation of IIa/IIc interconversion by smFRET(Figure 3a).[69] The model RNA interconverted spontaneously between FRET states consistent with stem IIc formation (with high E_{FRET}) and a cluster of FRET values consistent with stem IIa formation (with low to mid E_{FRET}) in the absence of other factors. This result suggests that unwinding of IIa or IIc by a helicase such as Prp5 is not required for their interconversion. While toggling of the stem II region between IIa and IIc occurred spontaneously, presence of physiologically relevant amounts of Mg^{2+} or the Cus2 protein strongly suppressed IIc and promoted IIa formation. The authors concluded from these observations that while Cus2 may bind stem IIc, the consequence of its interaction with stem II is to promote IIc destabilization or IIa formation. Furthermore, the spliceosome may need to interact with and stabilize stem IIc directly in order to prevent its spontaneous switching to IIa in the presence of Mg^{2+}. It is not known how spliceosome components interact with stem IIc during catalysis and the stem II region was not modeled in a recent structure of a spliceosomal complex isolated from *S. pombe*.[70] Significantly, it will be important, as with all model systems, to determine if results observed by Rodgers *et al.* on a small RNA fragment can be reproduced in the native complex. Thus, these smFRET results will likely form the basis for future structural and biochemical probing of the stem II region of U2 and its conformational control by the spliceosome.

Subsequent to spliceosome assembly and activation (Figure 1), the region of the U2 snRNA just 5' of stem II becomes basepaired with U6 to form part of the spliceosomal active site (U2/U6). The structure of U2/U6 has been a focus of research of many laboratories over the past few decades.[54,55,71,72] Genetic work indicated that U2/U6 adopted a 3-helix form necessary for both catalytic steps.[72,73] In contrast, NMR work revealed that a truncated, model U2/U6 duplex can also form a 4-helix structure in the absence of divalent metal ions or splicing proteins,[55] although data obtained by NMR and X-ray scattering of a larger U2/U6 model were consistent with the 3-helix conformation.[54] The cryo-EM structure of the *S. pombe* spliceosome lariat-intron product complex revealed a 3-helix conformation of U2/U6 consistent with genetic results but lacking U2/U6 helix III.[74]

It is possible that U2/U6 can adopt multiple conformations during distinct stages of splicing. Evidence for structural flexibility of U2/U6 has come from smFRET experiments by Guo *et al.* carried out with a model system for the yeast U2/U6 di-snRNA and in the absence of proteins.[75] For their model system, Guo *et al.* assembled 3 RNA oligos that together mimicked the proposed secondary structure of U2/U6 in the spliceosome. The smFRET data revealed three E_{FRET} states: a conformation proposed to represent the 4-helix structure with high FRET, a conformation proposed to represent the 3-helix structure with low FRET, and a novel structural intermediate between the two conformations and also with an intermediate FRET signal (Figure 3b). As with U2 stem II, interconversion between these RNA structures could be regulated by Mg^{2+} which favors the 3-helix structure. Guo and coworkers hypothesized that their observed dynamics may correspond to docking and undocking of functionally important parts of the U2/U6 RNA model into conformations similar to those required for catalysis in the spliceosome. Subsequent work by Karunatilaka and Rueda

showed that the structural transitions observed by Guo *et al.* using a yeast U2/U6 model are conserved in a model for human U2/U6.[76] While Mg^{2+} also promoted formation of a low FRET state and 3-helix structure in their human U2/U6 model, inclusion of post-transcriptional modifications in the RNAs did the opposite. 2'-*O*-methyl guanosine and pseudouridine incorporation into the U2 portion of the model stabilized the 4-helix structure, albeit by only fractions of a kcal/mol. Together these results suggest that the U2/U6 di-snRNA is inherently conformationally dynamic and responsive to the influence of Mg^{2+} and post-transcriptional modifications. It remains to be seen, however, if dynamic transitions between 3- and 4-helix conformations can be observed in intact spliceosomes by smFRET or by single particle cryo-EM structural elucidation.

Before U6 becomes basepaired to U2 to form the U2/U6 di-snRNA, it first must be released from U4 during spliceosomal activation (Figure 1). Spliceosomal activation is probably the most dramatic rearrangement in splicing and involves disruption of U4/U6 basepairing and expulsion of the U4 snRNA along with several U4- and U4/U6-snRNP proteins as the active site is formed.[1,5,77] Several groups have recently begun to study U4/U6 structure and dynamics in an effort to understand this transition. Both Hardin *et al.* and Cornilescu *et al.* used smFRET to study dynamics of a U4/U6 model di-RNA.[56,78] Both groups showed that the 3-helical junction formed by the RNA was remarkably static with little evidence for dynamics on the millisecond to minute timescale, in agreement with studies of other 3-helical junction RNAs.[79] Hardin *et al.* went on to propose that while the U4/U6 junction is static, the relative orientation of the U4 5' stem loop can change upon addition of various U4/U6 di-snRNP proteins with Prp31 promoting approach of the 5' stem loop towards U4/U6 stem II and Prp3 and Prp4 promoting an increase in 5' stem loop/ stem II distance (Figure 3c). The exact correlation of smFRET data with U4/U6 structure is unclear: Hardin *et al.* hypothesized that their smFRET data is consistent with co-axial stacking of U4/U6 stem I and stem II along with movement of this 5' stem loop. In contrast, Cornilescu *et al.* determined the structure of a U4/U6 model di-RNA by a combined NMR/X-ray scattering approach. The structure revealed that despite a rigid conformation, stem I and II are not co-axially stacked in the U4/U6 model. Cornilescu and coworkers' results require protein-dependent conformational change of U4/U6 stems I and II in order to transition the di-snRNA into the co-axially stacked conformation observed in the tri-snRNP cryo-EM structure.[80] In either case, both groups show that spliceosomal proteins likely dramatically impact U4/U6 structure and, consequently, removal of these proteins might be an important step in promoting U4/U6 unwinding and spliceosomal activation.

In addition to studies of snRNA dynamics, model systems combined with smFRET have also been able to shed light on interactions between protein splicing factors and RNAs. Lamichhane *et al.* have used a smFRET assay to show directly that a fragment of the alternative splicing factor polypyrimidine tract-binding protein (PTB) can alter RNA conformation.[81] A recent structure of PTB containing RNA recognition motifs (RRMs) 3 and 4, called PTB34, revealed that the RRMs are situated back-to-back with one another with the RNA binding sites facing outwards.[82] This structure suggested that these domains could facilitate looping of pre-mRNAs by PTB to sequester exons or BSs from the splicing machinery and regulate alternative splicing. To test this hypothesis, Lamichhane *et al.* developed a smFRET-based RNA looping assay (Figure 3d). These experiments showed

PTB34 can induce conformational changes in a tethered RNA molecule and bring distal fluorophores into close proximity. These smFRET results in combination with other data suggest that RNA looping by PTB likely represents a molecular mechanism for regulating alternative splicing.

Single Molecule Studies of Spliceosomes

In addition to model systems, single molecule fluorescence approaches have made important contributions towards understanding spliceosome biochemistry by analyzing intact, functional spliceosomes. Obtaining spliceosomes for single molecule analysis is quite challenging since spliceosome assembly and activation (Figure 1) cannot yet be reconstituted *in vitro*. To overcome this obstacle, several groups have developed methods for studying single spliceosomes either directly in unfractionated whole cell extract[28,83,84] or subsequent to purification.[85–88] The former method facilitates analysis of the earliest stages of spliceosome assembly and activation while the latter is useful in isolating activated spliceosomes poised for conversion into catalytic complexes.

Insights into Spliceosome Assembly from Single Molecule Colocalization—

Single molecule colocalization (Figure 2a, also called Colocalization Single Molecule Spectroscopy or CoSMoS) has proven valuable for studying a number of complex cellular machines including the spliceosome.[28,83,89–92] With CoSMoS, multiple components of the spliceosome can be monitored simultaneously with spectrally-distinguishable fluorophores. Spliceosomal complex formation can then be detected by appearance of colocalized spots of fluorescence from these components on surface tethered pre-mRNAs. This basic approach has provided insight into multiple aspects of spliceosome assembly. In initial experiments, Hoskins *et al.* were able to follow spliceosome assembly in real-time in yeast whole cell extract and directly observe reversible interactions of the U1, U2, U4/U6.U5 tri-snRNP, and NTC (Figure 1) with pre-mRNA substrates.[83] This data revealed that spliceosome assembly is a highly reversible process and that association of a particular factor does not commit the pre-mRNA to splicing, rather the probability of splicing occurring increases as spliceosome assembly progresses.

One key feature of the CoSMoS strategy developed by Hoskins *et al.* is that it does not rely on labeling pure proteins with fluorophores—endogenous spliceosome components can be labeled in yeast whole cell extract using chemical biology tools. To achieve this, yeast splicing factors were genetically fused to either *E. coli* dihydrofolate reductase or SNAP-tag proteins.[83,93] These small proteins facilitate specific labeling of splicing factors with bright fluorophores suitable for single molecule imaging. This tag-based labeling strategy is a pragmatic solution for preparing fluorescent proteins for single molecule colocalization experiments where fluorophore proximity and smFRET data collection are not concerns.

From these initial experiments, the CoSMoS approach has been extended in several ways to address particular aspects of splicing. Shcherbakova *et al.* used a creative fluorophore incorporation strategy to produce pre-mRNAs containing multiple intronic fluorophores.[89] Together with experiments in which the U1, U2, and tri-snRNP were all simultaneously labeled with fluorophores, Shcherbakova and coworkers were able to demonstrate that functional spliceosome assembly in yeast can occur via either U1- or U2-first pathways

(Figure 4a). Which pathway predominates is pre-mRNA sequence specific with some canonical *in vitro* yeast splicing substrates (ACT1 and RP51A) showing a strong preference for the U1-first pathway. By combining colocalization with smFRET (FRET-CoSMoS), Crawford *et al.* were able to correlate binding of spliceosomal components with conformational changes of the pre-mRNA substrate.[28] Surprisingly, these results showed that the 5' SS and BS do not become the most closely juxtaposed until very late in spliceosome assembly and soon after NTC association. This was surprising since crosslinking of human splicing complexes suggested that the sites of chemistry are brought together very early in spliceosome assembly.[94]

All of the above experiments rely on using CoSMoS to study splicing factors assembling on surface-tethered pre-mRNAs. To study interactions between splicing factors in the absence of spliceosome assembly, Rodgers *et al.* recently combined CoSMoS with Single Molecule Pull-down (SiMPull).[95,96] SiMPull methods enable capture and single-molecule characterization of cellular complexes from lysates by pull-down of FP-tagged molecules with antibodies directly onto glass microscope slides. Rodgers *et al.* optimized the SiMPull approach by developing SNAP-SiMPull to facilitate labeling and isolation of complexes from yeast extract. SNAP-SiMPull relies on bright, photostable organic fluorophores—an advantage compared to FPs which sometimes fail to mature and fluoresce when expressed in yeast.[96] To demonstrate the usefulness of this approach, Rodgers *et al.* used SNAP-SiMPull to label and isolate the branchpoint bridging protein (BBP) and study its interactions with RNAs as well as to demonstrate that an intact yeast U6 snRNA is required for colocalization of the Lsm and Prp24 proteins. This latter result suggests that U6 snRNP formation occurs in multiple steps and that the snRNA does not associate with a pre-assembled Lsm/Prp24 complex.

Insights into pre-mRNA Dynamics during Splicing from smFRET—

Understanding the conformational changes associated with the pre-mRNA substrate during splicing is critical for deciphering the catalytic mechanism of the spliceosome since proper juxtaposition of splice sites is critical for splicing chemistry to occur. In addition to the FRET-CoSMoS experiments by Crawford *et al.*, several other smFRET experiments have been used to analyze pre-mRNA conformational transitions that occur during splicing. By ingeniously selecting and engineering a small, model pre-mRNA,[97] Abelson *et al.* were able to demonstrate that the pre-mRNA interconverts reversibly through a number of conformational states throughout spliceosome assembly and splicing.[84] This result clearly demonstrated that pre-mRNA conformational changes during splicing are reversible and complement the reversible complex binding events observed by Hoskins *et al.* as well as biochemical evidence for reversible splicing chemistry.[98]

Extending from these studies, Krishnan *et al.* then were able to use smFRET in combination with affinity-purified spliceosomes stalled prior to 5' SS cleavage to study pre-mRNA rearrangements that precede catalysis.[85] In this case, spliceosomes were stalled using a temperature sensitive allele of the spliceosomal ATPase Prp2 (*prp2-1*)[99] that blocks the final stages of spliceosomal activation. Stalled spliceosomes were then pulled-down onto slides for smFRET analysis and could be pushed to subsequent stages in splicing by addition of recombinant proteins. These experiments revealed that juxtaposition of the BS and 5' SS

required ATP hydrolysis by Prp2, which likely remodels U2 proteins surrounding the BS to facilitate this conformational transition.[100–102] Since Prp2 associates subsequent to NTC binding, these results also clarified those obtained by Crawford *et al.* using FRET-CoSMoS. Furthermore, Krishnan *et al.* showed that while Prp2 activity is necessary for this structural rearrangement to occur, the spliceosomal product of Prp2 activity is very conformationally dynamic. A second protein, Cwc25, is required for 5' SS cleavage.[103] Based on smFRET data, Krishnan *et al.* propose that Cwc25 functions by stabilizing conformations in which the 5' SS and BS have been juxtaposed (Figure 4b). Together, Krishnan and coauthors hypothesized that the spliceosome may function as a biased Brownian ratchet with Cwc25 functioning as a "pawl" to bias spliceosomal conformation towards states compatible with 5' SS cleavage.

One aspect of studying spliceosomes compared to model systems is that the dynamic transitions and single molecule signals observed in spliceosomes can be extremely complicated. Blanco *et al.* developed a new approach for analyzing complex smFRET data sets obtained from studies of highly asynchronous and dynamic spliceosomes.[104] This approach utilizes clustering analysis of smFRET data analyzed by HMM to sort molecules based on common patterns of behavior (Single Molecule Cluster Analysis or SiMCAn). This method allowed Blanco *et al.* to rapidly analyze smFRET data collected from >10,000 pre-mRNAs under various conditions. By using SiMCAn in combination with pre-mRNA and ATPase mutants, Blanco *et al.* were able to identify a conformation specifically associated with a 3' SS mutant pre-mRNA that suggests that the splicing intermediate has been "undocked" from the active site as a consequence of spliceosomal proofreading.[8] Recently, this hypothesis has been significantly expanded by Semlow *et al.* using both bulk biochemical assays and smFRET analysis of stalled spliceosomes.[105] Semlow *et al.* propose that the spliceosomal DEAH-box ATPases function to dock and undock the pre-mRNA from the spliceosome active site to promote either progression through the splicing reaction or proofreading and discard. Significantly, this docking and undocking behavior also allows the spliceosome to sample alternative BS or 3' SS. These observations provide a mechanism for regulation of alternative splicing after spliceosome assembly and within catalytically activated spliceosomes.

Insights into Splicing Factor Dynamics from dcFCCS—The comings and goings of snRNPs and the NTC during spliceosome assembly represent only a small subset of the compositional changes occurring on the spliceosome. In addition to these large complexes, dozens of other proteins are transiently associating with the spliceosome at various stages. To study these transiently associated factors, Ohrt *et al.* used dcFCCS to study how splicing factors interact with purified spliceosomes stalled prior to either the first or second step of splicing.[86,87] In these experiments, spliceosomes were first assembled on an actin pre-mRNA substrate harboring a red-laser excitable Atto647N fluorophore installed via modification of a 5' terminal guanosine 5'-monophosphorthioate. Spliceosomes were poised at various stages by either using the same *prp2-1* mutation used by Krishnan *et al.* to block the final stages of spliceosome activation and 5' SS cleavage or by using a 3' SS mutation to block exon ligation. These stalled spliceosomes were then purified using preparative-scale affinity purification protocols developed by Lührmann and coworkers to isolate pure, well-

characterized complexes.[1,88] Significantly, the use of these purified and characterized complexes allowed Ohrt *et al*. to study binding interactions by adding back various splicing factors or ATP and by varying ionic strength, an approach that would have been extremely difficult to employ in cell extracts. To facilitate dcFCCS, a second fluorophore was then attached to a splicing factor either by genetic fusion to GFP or by chemically labeling a purified protein with a blue laser-excitable Alexa488 fluorophore. dcFCCS was used to detect and analyze single particles that contained either the labeled pre-mRNA, the labeled protein, or both the labeled pre-mRNA and protein.

The pragmatic use of GFP fusions allowed Ohrt *et al*. to study the binding interactions of a large number of splicing factors with these purified spliceosomes(Figure 4c).[86] Among their conclusions, Ohrt *et al*. were able to show that binding interactions of components of both U2 SF3a and SF3b to the spliceosome were weakened after the addition of Prp2, ATP, and Prp2's cofactor protein Spp2. This suggests that proteins near the intronic BS are remodeled just prior to catalysis, likely to facilitate active site formation and in agreement with results using other techniques.[100,101] The weakened interaction may also explain variable results in isolating spliceosomes containing the SF3 complex—dynamic binding interactions of SF3 may result in its dissociation under certain purification conditions and not others or when certain spliceosomal complexes are isolated.[1,70,100,106] In addition to weakening SF3 interactions, Ohrt and coworkers were also able to demonstrate that Prp2 activity results in creation of a high affinity binding site for Cwc25—the protein Krishnan *et al*. suggest acts as a "pawl" to bias the spliceosome towards a catalytic conformation. Thus, it is likely that Prp2 activity results in active site remodeling that either directly or indirectly weakens binding interactions between the spliceosome and some proteins (the SF3 complex) while strengthening interactions with others (Cwc25).

In a second set of experiments, Ohrt *et al*. were able to use a similar dcFCCS-based strategy to study the transition of the spliceosome between the first (5' SS cleavage) and second (exon ligation) steps of splicing.[87] Ohrt and coworkers discovered that an additional consequence of Prp2 activity is creation of low-affinity binding sites for the second step splicing factors Prp16, Slu7, and Prp18[107,108] on the spliceosome prior to catalysis. After 5' SS cleavage, Prp16 binds with higher affinity, likely reflecting its role in supporting the spliceosome's transition to catalysis of exon ligation. Exon ligation itself is promoted by Cwc25 departure, the same protein recruited by Prp2 activity and that promotes 5' SS cleavage. Combined these results suggest a model in which Cwc25 and Slu7/Prp18 have parallel roles in stabilizing spliceosomal conformations competent for the first and second steps of splicing, respectively, and that Cwc25 must be removed for Slu7 and Prp18 to fulfill their function.

Single Molecule Studies of Splicing in Cells

A major challenge for future single molecule studies of the spliceosome is to study this macromolecular machine *in situ* while it is splicing in the cell. These experiments are critical for understanding how the spliceosome operates in its native biological context—not just within the nucleus but also coupled with other steps in gene expression.[109] Single molecule imaging of spliceosomes has not yet been achieved in cells, and this will be a formidable

challenge given the high concentration of splicing factors within the nucleus—although recent advances in microscopic imaging of fluorophore-dense samples do show some promise.[31] Several groups have already made great strides in using single molecule methods (Figure 2c) to study the splicing of single pre-mRNA transcripts in cells rather than single spliceosomes themselves. In all cases splicing chemistry *per se* is not detected, rather colocalization of fluorescent signals from exons and introns is used as a proxy for the presence of pre-mRNA or introns while exon fluorescence in the absence of intron fluorescence is a proxy for mRNA formation. While current methods cannot yet distinguish between unspliced transcripts and spliced mRNA and lariat-intron products still simultaneously bound to spliceosomes, they have proven valuable in understanding the coupling between transcription and the splicing and release of product mRNAs.

Single Molecule Studies of Splicing in Fixed Cells

Using smFISH, Vargas *et al.* studied the splicing of several reporter genes in mammalian and *Drosophila* cells.[110] To image single molecules and confirm the presence of an intron, each transcript was targeted with 32–384 fluorophores that allowed the RNA to be visualized as a single bright spot by wide-field microscopy (Figures 5a,b). This high labeling density was achieved in some experiments by insertion of tandem arrays of selected sequences into the intron and 3' untranslated region (UTR) of a reporter gene. By using two different arrays, pre-mRNAs (or spliceosome-bound products) could be detected by colocalization of spots originating from the intronic array with spots originating from the 3' UTR. These colocalized signals were mostly present near the sites of transcription. In contrast, mRNAs could be detected by observing spots of 3' UTR fluorescence without any colocalized intronic signal, and spliced introns could be detected by observing spots of intronic fluorescence without any colocalized 3' UTR signal (Figure 5b). As expected, mRNA spots were mostly present in the cytosol, with a few imaged within the nucleus. Intron-only spots were present exclusively within the nucleus. Fortuitously, Vargas *et al.* discovered that one of their tandem arrays was able to uncouple transcription from splicing—transcripts containing this intronic array sequence could be detected in the nucleoplasm not just at the transcriptional locus. This discovery allowed Vargas *et al.* to determine that splicing could be uncoupled from transcription by sequestration of an intron's polypyrimidine tract and that other well-studied examples of alternative splicing regulation (*Drosophila Sxl*-dependent splicing and human PTB-dependent splicing of the neuronal PTB-gene) also induce decoupling. In sum, Vargas and coworkers' results support regulation of alternative splicing through control of coupling between splicing and transcription.

Single Molecule Studies of Splicing in Live Cells

Recently, experiments aimed at analyzing the coupling of splicing and transcription on single transcripts have been carried out in live cells by two groups using MS2-based labeling strategies to decorate RNAs with dozens of fluorescent proteins.[111,112] These experiments followed transcription and splicing in real time and provided substantial new insights into the kinetics of these steps in gene expression. On a fundamental level, both groups also relied on a colocalization strategy similar to that employed by Vargas *et al.* Intron-containing transcripts were detected by colocalization of a fluorescent spot originating from an intron

with a fluorescence spot originating from elsewhere on the transcript (in the 3' UTR in the case of Coulon *et al.* and in a downstream intron in the case of Martin *et al.*).

In their experiments, Coulon and coworkers used a human β-globin reporter gene containing a 24xPP7 hairpin cassette in the second intron and a 24xMS2 hairpin cassette in the 3' UTR.[111] This enabled intron labeling with a PP7-mCherry FP and 3' UTR labeling with MS2-GFP (Figure 5c). The reporter gene was then stably integrated into U2-OS cells, and movies were recorded following GFP and mCherry fluorescence. During transcription, spots of mCherry and GFP fluorescence appeared at the same locations right after one another, indicative of transcription of the labeled intronic region followed by the 3' exon and UTR (Figure 5d). Signals disappeared as the RNA products were released from the transcriptional locus and began rapidly diffusing throughout the nucleoplasm. In some cases the intronic signal disappeared prior to the 3' UTR signal, consistent with co-transcriptional splicing and release of the transcript from the spliceosomal product complex (*i.e.*, spliced product release). In other cases, both signals disappeared simultaneously consistent with release of either unspliced pre-mRNA or transcripts still bound by an intron-lariat-containing spliceosome.

To further analyze the kinetics of splicing and transcription, Coulon *et al.* used correlation analysis (similar to methods used in dcFCCS) to study the time dependent changes in the intronic and 3' UTR signals.[111] Using this technique they found that both co-transcriptional and post-transcriptional spliced product release occur stochastically due to kinetic competition between competing pathways. The majority of spliced product release occurs after transcription has stopped and may not be completed before transcript release from chromatin. Surprisingly, spliced product release was relatively slow when the transcript remained bound to chromatin with a mean intron lifetime of ~4.5min compared to the transcriptional elongation rate of ~2.6 kb/min. Both small molecule spliceosome inhibitors and cancer-associated mutations in the splicing factor U2AF1 caused a decrease in the rate of spliced product release and the fraction of this release that occurred while the RNA was still associated with the transcriptional locus. In contrast, once the transcript had been released from chromatin, the intronic signal was lost very quickly (~13s). This latter result suggests that, at minimum, the completion of splicing by mRNA product release may occur quite rapidly in the nucleoplasm.

Interestingly, Martin *et al.* used a similar single-molecule approach to also study the transcription and splicing of a human β-globin reporter gene, this time containing 24xMS2 and 25xλN stem loops in the first or second intron.[112] Rather than use U2-OS cells, Martin *et al.* stably integrated their reporter into HEK293 cells using the site-specific recombinase Flp to create a library of cells each containing a single version of the reporter gene integrated into the same chromosomal location. By measuring fluctuations in fluorescence intensity, they calculated intron lifetimes of ~20 and 30s for the first and second intron, respectively, with most intron signal loss events occurring near the site of transcription and the splicing of the first exon pair preceding the splicing of the second. By using a similarly constructed mouse IgM reporter pre-mRNA, Martin and colleagues were also able to show that the rates of intron loss were responsive to sequences within the intron: transcripts harboring weak polypyrmidine tracts in between the BS and 3' SS lost intron signals more slowly than those

harboring strong polypyrmidine tracts. Together, these results suggest 10-fold faster rates of splicing compared to those obtained by Coulon *et al*. as well as tighter coupling between transcription and splicing. Indeed, Martin *et al*. speculate that the transcription may be rate-limiting for splicing *in vivo*. The origin of the differences in kinetics obtained by Coulon *et al*. and Martin *et al*. has not yet been resolved; however, given the flexibility of the splicing machinery, it is likely that the interconnectedness of steps in RNA processing could be sensitive to cell type, the surrounding chromatin environment of a given gene, and the transcript sequence itself. Subtle changes in any of these factors may potentially shift the balance between co- and post-transcriptional splicing and mRNA release from the spliceosome.

In addition to observing the pre-mRNA substrate, it is also possible to use single molecule approaches to observe and obtain kinetic data from protein splicing factors in live cells. FCS experiments by Huranová *et al*. have revealed the *in vivo* dynamics of a number of GFP-tagged snRNP proteins.[39,113,114] These experiments revealed that several snRNP proteins likely exist in two pools both in the nucleoplasm and in splicing factor compartments ("nuclear speckles"). A fast moving portion likely represents free proteins not yet assembled into snRNPs; in contrast a much slower moving portion likely represents proteins incorporated into snRNPs and splicing complexes. Interestingly, Huranová *et al*. were able to use this same set of GFP-tagged splicing factors to study slower events using fluorescence recovery after photobleaching (FRAP). The FRAP data represents the average diffusive behavior of a large number of GFP-tagged splicing factors and can be used to deduce both diffusion and binding parameters. With the assumption that most snRNPs in the nucleoplasm are participating in splicing, Huranová *et al*. constructed a kinetic model for spliceosome assembly and release of snRNPs during splicing. They predict that the U2 and U5 snRNPs engage transcripts for ~15–30s and that most splicing reactions would be complete within 30s. These data are closer in agreement to the *in vivo* splicing kinetics reported by Martin *et al*. and suggest that illumination of the splicing reaction in cells may benefit from multiple, complementary microscopic approaches to monitor both transcript and snRNP dynamics.

Conclusion

To date, single molecule fluorescence studies have provided insight into numerous facets of spliceosome biochemistry. Luckily for those interested in using single molecule approaches to study splicing, many outstanding questions yet remain. Foremost is to make use of the avalanche of structural information on the spliceosome that has recently been obtained using X-ray crystallography and cryo-electron microscopy.[53,59,70,80,115,116,117] These new structures provide staggering snapshots of the scope of the conformational changes spliceosomes undergo to bring about splicing. For example, recent structures of the core U6 snRNP from *S. cerevisiae*,[53] the *S. cerevisiae* U4/U6.U5 tri-snRNP,[80] and a U2/U6.U5 spliceosome from *S. pombe*[70] reveal the dramatic conformational changes taking place within the U6 snRNA (Figure 6). Understanding the dynamic transitions of U6 as it progresses between these various complexes will likely require single molecule approaches among many other methods. Single molecule tools will also prove valuable in testing hypotheses related to individual complexes as well. Based on the *S. pombe* structure alone, single molecule methods could be useful in deducing changes in active site dynamics in the

spliceosome as a consequence of Drn1/Cwf19 association, understanding Prp8 domain flexibility, or if the observed spliceosome architecture is conserved in other post-activation spliceosomal complexes as has been hypothesized.[74]

A second major area of focus for future single molecule fluorescence experiments is complementing work carried out in *S. cerevisiae* with experiments on human spliceosomes. Not only are *in vitro* experiments with the human splicing machinery critical for understanding processes not represented in the yeast spliceosome (such as exon junction complex deposition or the role of arginine-serine (RS) domains in stabilizing certain interactions), single molecule experiments in cells will greatly complement data obtained by next-generation sequencing (NGS) methods that reveal unexpected complexities in splicing regulation and coupling with transcription.[118–121] Already some laboratories are using single molecule fluorescence tools to study the human splicing machinery *in vitro*[122] and related methods such as fluorescence lifetime imaging microscopy (FLIM) have proven useful for identifying and studying splicing factor complexes in live cells.[123] In the new era of spliceosome structures and NGS analysis of spliceosome activity, the future for single molecule studies of the spliceosome looks very bright. It is time for the spliceosome to shine!

Acknowledgments

ACD, ISN, and AAH acknowledge support from startup funding from the University of Wisconsin-Madison, Wisconsin Alumni Research Foundation (WARF), and the Department of Biochemistry, awards from the National Institutes of Health (R00 GM086471, R01 GM112735), the Arnold and Mabel Beckman Foundation, and the Shaw Scientist Program of the Greater Milwaukee Foundation. We thank Laura Vanderploeg (UW Dept. of Biochemistry) for help in figure creation and K. Nagai for providing PDB coordinates of the *S. cerevisiae* tri-snRNP.

References

1. Fabrizio P, Dannenberg J, Dube P, Kastner B, Stark H, Urlaub H, Lührmann R. The evolutionarily conserved core design of the catalytic activation step of the yeast spliceosome. Mol Cell. 2009; 36:593–608. [PubMed: 19941820]
2. Jurica MS, Moore MJ. Pre-mRNA splicing: awash in a sea of proteins. Mol Cell. 2003; 12:5–14. [PubMed: 12887888]
3. Matlin AJ, Clark F, Smith CWJ. Understanding alternative splicing: towards a cellular code. Nat Rev Mol Cell Biol. 2005; 6:386–398. [PubMed: 15956978]
4. Chen C, Greenberg MJ, Laakso JM, Ostap EM, Goldman YE, Shuman H. Kinetic schemes for post-synchronized single molecule dynamics. Biophys J. 2012; 102:L23–L25. [PubMed: 22455931]
5. Wahl MC, Will CL, Lührmann R. The spliceosome: design principles of a dynamic RNP machine. Cell. 2009; 136:701–718. [PubMed: 19239890]
6. Papasaikas P, Valcárcel J. The Spliceosome: The Ultimate RNA Chaperone and Sculptor. Trends in Biochemical Sciences. 2015; 41:33–45. [PubMed: 26682498]
7. Staley JP, Guthrie C. Mechanical devices of the spliceosome: motors, clocks, springs, and things. Cell. 1998; 92:315–326. [PubMed: 9476892]
8. Semlow DR, Staley JP. Staying on message: ensuring fidelity in pre-mRNA splicing. Trends in Biochemical Sciences. 2012; 37:263–273. [PubMed: 22564363]
9. Gell, C.; Brockwell, D.; Smith, A. Handbook of Single Molecule Fluorescence Spectroscopy. Oxford: Oxford University Press; 2013.
10. Larson J, Kirk M, Drier EA, O'Brien W, MacKay JF, Friedman LJ, Hoskins AA. Design and construction of a multiwavelength, micromirror total internal reflectance fluorescence microscope. Nat Protoc. 2014; 9:2317–2328. [PubMed: 25188633]

11. Larson JD, Rodgers ML, Hoskins AA. Visualizing cellular machines with colocalization single molecule microscopy. Chem Soc Rev. 2014; 43:1189–1200. [PubMed: 23970346]
12. Friedman LJ, Chung J, Gelles J. Viewing dynamic assembly of molecular complexes by multi-wavelength single-molecule fluorescence. Biophys J. 2006; 91:1023–1031. [PubMed: 16698779]
13. Zhao R, Rueda D. RNA folding dynamics by single-molecule fluorescence resonance energy transfer. Methods. 2009; 49:112–117. [PubMed: 19409995]
14. Selvin, PR.; Ha, T. A Laboratory Manual. New York: Cold Spring Harbor Laboratory Press; 2008. Single-Molecule Techniques.
15. Cohen AE, Moerner WE. Suppressing Brownian motion of individual biomolecules in solution. Proc Natl Acad Sci USA. 2006; 103:4362–4365. [PubMed: 16537418]
16. Leslie SR, Fields AP, Cohen AE. Convex lens-induced confinement for imaging single molecules. Anal Chem. 2010; 82:6224–6229. [PubMed: 20557026]
17. Tyagi S, VanDelinder V, Banterle N, Fuertes G, Milles S, Agez M, Lemke EA. Continuous throughput and long-term observation of single-molecule FRET without immobilization. Nat Meth. 2014; 11:297–300.
18. Walter NG, Huang CY, Manzo AJ, Sobhy MA. Do-it-yourself guide: how to use the modern single-molecule toolkit. Nat Meth. 2008; 5:475–489.
19. Ha T, Enderle T, Ogletree DF, Chemla DS, Selvin PR, Weiss S. Probing the interaction between two single molecules: fluorescence resonance energy transfer between a single donor and a single acceptor. Proc Natl Acad Sci USA. 1996; 93:6264–6268. [PubMed: 8692803]
20. Kalinin S, Peulen T, Sindbert S, Rothwell PJ, Berger S, Restle T, Goody RS, Gohlke H, Seidel CAM. A toolkit and benchmark study for FRET-restrained high-precision structural modeling. Nat Meth. 2012; 9:1218–1225.
21. Muschielok A, Andrecka J, Jawhari A, Brückner F, Cramer P, Michaelis J. A nano-positioning system for macromolecular structural analysis. Nat Meth. 2008; 5:965–971.
22. Ouellet J, Schorr S, Iqbal A, Wilson TJ, Lilley DMJ. Orientation of cyanine fluorophores terminally attached to DNA via long, flexible tethers. Biophys J. 2001; 101:1148–1154. [PubMed: 21889452]
23. Lee NK, Kapanidis AN, Wang Y, Michalet X, Mukhopadhyay J, Ebright RH, Weiss S. Accurate FRET measurements within single diffusing biomolecules using alternating-laser excitation. Biophys J. 2005; 88:2939–2953. [PubMed: 15653725]
24. Mckinney SA, Joo C, Ha T. Analysis of single-molecule FRET trajectories using hidden Markov modeling. Biophys J. 2006; 91:1941–1951. [PubMed: 16766620]
25. Blanco M, Walter NG. Analysis of complex single-molecule FRET time trajectories. Meth Enzymol. 2010; 472:153–178. [PubMed: 20580964]
26. Bronson JE, Fei J, Hofman JM, Gonzalez RL, Wiggins CH. Learning rates and states from biophysical time series: a Bayesian approach to model selection and single-molecule FRET data. Biophys J. 2009; 97:3196–3205. [PubMed: 20006957]
27. Friedman LJ, Gelles J. Multi-wavelength single-molecule fluorescence analysis of transcription mechanisms. Methods. 2015; 86:27–36. [PubMed: 26032816]
28. Crawford DJ, Hoskins AA, Friedman LJ, Gelles J, Moore MJ. Single-molecule colocalization FRET evidence that spliceosome activation precedes stable approach of 5’ splice site and branch site. Proc Natl Acad Sci USA. 2013; 110:6783–6788. [PubMed: 23569281]
29. Weidemann T, Schwille P. Dual-color fluorescence cross-correlation spectroscopy with continuous laser excitation in a confocal setup. Meth Enzymol. 2013; 518:43–70. [PubMed: 23276535]
30. Huang B, Babcock H, Zhuang X. Breaking the diffraction barrier: super-resolution imaging of cells. Cell. 2010; 143:1047–1058. [PubMed: 21168201]
31. Liu Z, Lavis LD, Betzig E. Imaging live-cell dynamics and structure at the single-molecule level. Mol Cell. 2015; 58:644–659. [PubMed: 26000849]
32. Pitchiaya S, Krishnan V, Custer TC, Walter NG. Dissecting non-coding RNA mechanisms in cellulo by Single-molecule High-Resolution Localization and Counting. Methods. 2013; 63:188–199. [PubMed: 23820309]

33. Pitchiaya S, Heinicke LA, Custer TC, Walter NG. Single Molecule Fluorescence Approaches Shed Light on Intracellular RNAs. Chem. Rev. 2014; 114:3224–3265. [PubMed: 24417544]
34. König I, Zarrine-Afsar A, Aznauryan M, Soranno A, Wunderlich B, Dingfelder F, Stüber JC, Plückthun A, Nettels D, Schuler B. Single-molecule spectroscopy of protein conformational dynamics in live eukaryotic cells. Nat Meth. 2015; 12:773–779.
35. Farlow J, Seo D, Broaders KE, Taylor MJ, Gartner ZJ, Jun YW. Formation of targeted monovalent quantum dots by steric exclusion. Nat Meth. 2013; 10:1203–1205.
36. Blehm BH, Schroer TA, Trybus KM, Chemla YR, Selvin PR. In vivo optical trapping indicates kinesin's stall force is reduced by dynein during intracellular transport. Proc Natl Acad Sci USA. 2013; 110:3381–3386. [PubMed: 23404705]
37. Liu Z, Legant WR, Chen BC, Li L, Grimm JB, Lavis LD, Betzig E, Tjian R. 3D imaging of Sox2 enhancer clusters in embryonic stem cells. Elife. 2014; 3:e04236. [PubMed: 25537195]
38. Zhao ZW, Roy R, Gebhardt JCM, Suter DM, Chapman AR, Xie XS. Spatial organization of RNA polymerase II inside a mammalian cell nucleus revealed by reflected light-sheet superresolution microscopy. Proc Natl Acad Sci USA. 2014; 111:681–686. [PubMed: 24379392]
39. Huranová M, Ivani I, Benda A, Poser I, Brody Y, Hof M, Shav-Tal Y, Neugebauer KM, Staněk D. The differential interaction of snRNPs with pre-mRNA reveals splicing kinetics in living cells. J Gen Physiol. 2010; 191:75–86.
40. Tyagi S. Imaging intracellular RNA distribution and dynamics in living cells. Nat Meth. 2009; 6:331–338.
41. Zenklusen D, Singer RH. Analyzing mRNA expression using single mRNA resolution fluorescent in situ hybridization. Meth Enzymol. 2010; 470:641–659. [PubMed: 20946829]
42. Femino AM, Fay FS, Fogarty K, Singer RH. Visualization of single RNA transcripts in situ. Science. 1998; 280:585–590. [PubMed: 9554849]
43. Raj A, van den Bogaard P, Rifkin SA, van Oudenaarden A, Tyagi S. Imaging individual mRNA molecules using multiple singly labeled probes. Nat Meth. 2008; 5:877–879.
44. Lubeck E, Cai L. Single-cell systems biology by super-resolution imaging and combinatorial labeling. Nat Meth. 2012; 9:743–748.
45. Chen KH, Boettiger AN, Moffitt JR, Wang S, Zhuang X. Spatially resolved, highly multiplexed RNA profiling in single cells. Science. 2015; 348 aaa6090.
46. Bertrand E, Chartrand P, Schaefer M, Shenoy SM, Singer RH, Long RM. Localization of ASH1 mRNA particles in living yeast. Mol Cell. 1998; 2:437–445. [PubMed: 9809065]
47. Wu B, Chao JA, Singer RH. Fluorescence Fluctuation Spectroscopy Enables Quantitative Imaging of Single mRNAs in Living Cells. Biophys J. 2012; 102:2936–2944. [PubMed: 22735544]
48. Daigle N, Ellenberg J. LambdaN-GFP: an RNA reporter system for live-cell imaging. Nat Meth. 2007; 4:633–636.
49. Smith DJ, Konarska MM. A critical assessment of the utility of protein-free splicing systems. RNA. 2009; 15:1–3. [PubMed: 19029306]
50. Smith DJ, Konarska MM. Identification and characterization of a short 2"-3" bond-forming ribozyme. RNA. 2009; 15:8–13. [PubMed: 19029304]
51. Valadkhan S, Manley JL. The use of simple model systems to study spliceosomal catalysis. RNA. 2009; 15:4–7. [PubMed: 19029305]
52. Valadkhan S, Manley JL. Splicing-related catalysis by protein-free snRNAs. Nature. 2001; 413:701–707. [PubMed: 11607023]
53. Montemayor EJ, Curran EC, Liao HH, Andrews KL, Treba CN, Butcher SE, Brow DA. Core structure of the U6 small nuclear ribonucleoprotein at 1.7-Å resolution. Nat Struct Mol Biol. 2014; 21:544–551. [PubMed: 24837192]
54. Burke JE, Sashital DG, Zuo X, Wang YX, Butcher SE. Structure of the yeast U2/U6 snRNA complex. RNA. 2012; 18:673–683. [PubMed: 22328579]
55. Sashital DG, Cornilescu G, McManus CJ, Brow DA, Butcher SE. U2-U6 RNA folding reveals a group II intron-like domain and a four-helix junction. Nat Struct Mol Biol. 2004; 11:1237–1242. [PubMed: 15543154]

56. Cornilescu G, Didychuk AL, Rodgers ML, Michael LA, Burke JE, Montemayor EJ, Hoskins AA, Butcher SE. Structural analysis of multi-helical RNAs by NMR-SAXS/WAXS: Application to the U4/U6 di-snRNA. J. Mol. Biol. 2016; 428:777–789. [PubMed: 26655855]
57. Sashital DG, Allmann AM, Van Doren SR, Butcher SE. Structural basis for a lethal mutation in U6 RNA. Biochemistry. 2003; 42:1470–1477. [PubMed: 12578359]
58. Sashital DG, Venditti V, Angers CG, Cornilescu G, Butcher SE. Structure and thermodynamics of a conserved U2 snRNA domain from yeast and human. RNA. 2007; 13:328–338. [PubMed: 17242306]
59. Kondo Y, Oubridge C, van Roon AMM, Nagai K. Crystal structure of human U1 snRNP, a small nuclear ribonucleoprotein particle, reveals the mechanism of 5' splice site recognition. Elife. 2015; 4:e04986.
60. Jacewicz A, Chico L, Smith P, Schwer B, Shuman S. Structural basis for recognition of intron branchpoint RNA by yeast Msl5 and selective effects of interfacial mutations on splicing of yeast pre-mRNAs. RNA. 2015; 21:401–414. [PubMed: 25587180]
61. Zhang ZM, Yang F, Zhang J, Tang Q, Li J, Gu J, Zhou J, Xu YZ. Crystal Structure of Prp5p Reveals Interdomain Interactions that Impact Spliceosome Assembly. Cell Reports. 2013; 5:1269–1278. [PubMed: 24290758]
62. Tanaka N, Schwer B. Characterization of the NTPase, RNA-binding, and RNA helicase activities of the DEAH-box splicing factor Prp22. Biochemistry. 2005; 44:9795–9803. [PubMed: 16008364]
63. Mozaffari-Jovin S, Santos KF, Hsiao HH, Will CL, Urlaub H, Wahl MC, Lührmann R. The Prp8 RNase H-like domain inhibits Brr2-mediated U4/U6 snRNA unwinding by blocking Brr2 loading onto the U4 snRNA. Genes Dev. 2012; 26:2422–2434. [PubMed: 23124066]
64. Mozaffari-Jovin S, Wandersleben T, Santos KF, Will CL, Lührmann R, Wahl MC. Novel regulatory principles of the spliceosomal Brr2 RNA helicase and links to retinal disease in humans. RNA Biol. 2014; 11:298–312. [PubMed: 24643059]
65. Weber G, Cristão VF, Alves F de L, Santos KF, Holton N, Rappsilber J, Beggs JD, Wahl MC. Mechanism for Aar2p function as a U5 snRNP assembly factor. Genes Dev. 2011; 25:1601–1612. [PubMed: 21764848]
66. Perriman RJ, Ares M. Rearrangement of competing U2 RNA helices within the spliceosome promotes multiple steps in splicing. Genes Dev. 2007; 21:811–820. [PubMed: 17403781]
67. Hilliker AK, Mefford MA, Staley JP. U2 toggles iteratively between the stem IIa and stem IIc conformations to promote pre-mRNA splicing. Genes Dev. 2007; 21:821–834. [PubMed: 17403782]
68. Liang WW, Cheng SC. A novel mechanism for Prp5 function in prespliceosome formation and proofreading the branch site sequence. Genes Dev. 2015; 29:81–93. [PubMed: 25561497]
69. Rodgers ML, Tretbar US, DeHaven A, Alwan AA, Luo G, Mast HM, Hoskins AA. Conformational dynamics of stem II of the U2 snRNA. RNA. 2016; 22:1–12. [PubMed: 26577377]
70. Yan C, Hang J, Wan R, Huang M, Wong CCL, Shi Y. Structure of a yeast spliceosome at 3.6-angstrom resolution. Science. 2015; 349:1182–1191. [PubMed: 26292707]
71. Sun JS, Manley JL. A novel U2-U6 snRNA structure is necessary for mammalian mRNA splicing. Genes Dev. 1995; 9:843–854. [PubMed: 7705661]
72. Madhani HD, Guthrie C. A novel base-pairing interaction between U2 and U6 snRNAs suggests a mechanism for the catalytic activation of the spliceosome. Cell. 1992; 71:803–817. [PubMed: 1423631]
73. Hilliker AK, Staley JP. Multiple functions for the invariant AGC triad of U6 snRNA. RNA. 2004; 10:921–928. [PubMed: 15146076]
74. Hang J, Wan R, Yan C, Shi Y. Structural basis of pre-mRNA splicing. Science. 2015; 349:1191–1198. [PubMed: 26292705]
75. Guo Z, Karunatilaka KS, Rueda D. Single-molecule analysis of protein-free U2-U6 snRNAs. Nat Struct Mol Biol. 2009; 16:1154–1159. [PubMed: 19881500]
76. Karunatilaka KS, Rueda D. Post-transcriptional modifications modulate conformational dynamics in human U2-U6 snRNA complex. RNA. 2013; 20:1–8. [PubMed: 24255166]
77. Brow DA. Allosteric cascade of spliceosome activation. Annu Rev Genet. 2002; 36:333–360. [PubMed: 12429696]

78. Hardin JW, Warnasooriya C, Kondo Y, Nagai K, Rueda D. Assembly and dynamics of the U4/U6 di-snRNP by single-molecule FRET. Nucleic Acids Res. 2015; 43:10963–10974. [PubMed: 26503251]

79. Ouellet J, Melcher S, Iqbal A, Ding Y, Lilley DMJ. Structure of the three-way helical junction of the hepatitis C virus IRES element. RNA. 2010; 16:1597–1609. [PubMed: 20581129]

80. Nguyen THD, Galej WP, Bai XC, Savva CG, Newman AJ, Scheres SHW, Nagai K. The architecture of the spliceosomal U4/U6.U5 tri-snRNP. Nature. 2015; 523:47–52. [PubMed: 26106855]

81. Lamichhane R, Daubner GM, Thomas-Crusells J, Auweter SD, Manatschal C, Austin KS, Valniuk O, Allain FHT, Rueda D. RNA looping by PTB: Evidence using FRET and NMR spectroscopy for a role in splicing repression. Proc Natl Acad Sci USA. 2010; 107:4105–4110. [PubMed: 20160105]

82. Oberstrass FC, Auweter SD, Erat M, Hargous Y, Henning A, Wenter P, Reymond L, Amir-Ahmady B, Pitsch S, Black DL, Allain FHT. Structure of PTB bound to RNA: specific binding and implications for splicing regulation. Science. 2005; 309:2054–2057. [PubMed: 16179478]

83. Hoskins AA, Friedman LJ, Gallagher SS, Crawford DJ, Anderson EG, Wombacher R, Ramirez N, Cornish VW, Gelles J, Moore MJ. Ordered and dynamic assembly of single spliceosomes. Science. 2011; 331:1289–1295. [PubMed: 21393538]

84. Abelson J, Blanco M, Ditzler MA, Fuller F, Aravamudhan P, Wood M, Villa T, Ryan DE, Pleiss JA, Maeder C, Guthrie C, Walter NG. Conformational dynamics of single pre-mRNA molecules during in vitro splicing. Nat Struct Mol Biol. 2010; 17:504–512. [PubMed: 20305654]

85. Krishnan R, Blanco MR, Kahlscheuer ML, Abelson J, Guthrie C, Walter NG. Biased Brownian ratcheting leads to pre-mRNA remodeling and capture prior to first-step splicing. Nat Struct Mol Biol. 2013; 20:1450–1457. [PubMed: 24240612]

86. Ohrt T, Prior M, Dannenberg J, Odenwälder P, Dybkov O, Rasche N, Schmitzová J, Gregor I, Fabrizio P, Enderlein J, Lührmann R. Prp2-mediated protein rearrangements at the catalytic core of the spliceosome as revealed by dcFCCS. RNA. 2012; 18:1244–1256. [PubMed: 22535589]

87. Ohrt T, Odenwälder P, Dannenberg J, Prior M, Warkocki Z, Schmitzová J, Karaduman R, Gregor I, Enderlein J, Fabrizio P, Lührmann R. Molecular dissection of step 2 catalysis of yeast pre-mRNA splicing investigated in a purified system. RNA. 2013; 19:902–915. [PubMed: 23685439]

88. Warkocki Z, Odenwälder P, Schmitzová J, Platzmann F, Stark H, Urlaub H, Ficner R, Fabrizio P, Lührmann R. Reconstitution of both steps of Saccharomyces cerevisiae splicing with purified spliceosomal components. Nat Struct Mol Biol. 2009; 16:1237–1243. [PubMed: 19935684]

89. Shcherbakova I, Hoskins AA, Friedman LJ, Serebrov V, Corrêa IR, Xu MQ, Gelles J, Moore MJ. Alternative Spliceosome Assembly Pathways Revealed by Single-Molecule Fluorescence Microscopy. Cell Reports. 2013; 5:151–165. [PubMed: 24075986]

90. Ticau S, Friedman LJ, Ivica NA, Gelles J, Bell SP. Single-Molecule Studies of Origin Licensing Reveal Mechanisms Ensuring Bidirectional Helicase Loading. Cell. 2015; 161:513–525. [PubMed: 25892223]

91. Friedman LJ, Gelles J. Mechanism of transcription initiation at an activator-dependent promoter defined by single-molecule observation. Cell. 2012; 148:679–689. [PubMed: 22341441]

92. Smith BA, Padrick SB, Doolittle LK, Daugherty-Clarke K, Corrêa IR, Xu MQ, Goode BL, Rosen MK, Gelles J, Sundquist W. Three-color single molecule imaging shows WASP detachment from Arp2/3 complex triggers actin filament branch formation. Elife. 2013; 2:e01008. [PubMed: 24015360]

93. Anderson EG, Hoskins AA. Single molecule approaches for studying spliceosome assembly and catalysis. Methods Mol Biol. 2014; 1126:217–241. [PubMed: 24549668]

94. Kent OA, MacMillan AM. Early organization of pre-mRNA during spliceosome assembly. Nat Struct Biol. 2002; 9:576–581. [PubMed: 12091875]

95. Jain A, Liu R, Ramani B, Arauz E, Ishitsuka Y, Ragunathan K, Park J, Chen J, Xiang YK, Ha T. Probing cellular protein complexes using single-molecule pull-down. Nature. 2011; 473:484–488. [PubMed: 21614075]

96. Rodgers ML, Paulson J, Hoskins AA. Rapid isolation and single-molecule analysis of ribonucleoproteins from cell lysate by SNAP-SiMPull. RNA. 2015; 21:1031–1041. [PubMed: 25805862]

97. Abelson J, Hadjivassiliou H, Guthrie C. Preparation of fluorescent pre-mRNA substrates for an smFRET study of pre-mRNA splicing in yeast. Meth Enzymol. 2010; 472:31–40. [PubMed: 20580958]

98. Tseng CK, Cheng SC. Both catalytic steps of nuclear pre-mRNA splicing are reversible. Science. 2008; 320:1782–1784. [PubMed: 18583613]

99. Vijayraghavan U, Company M, Abelson J. Isolation and characterization of pre-mRNA splicing mutants of Saccharomyces cerevisiae. Genes Dev. 1989; 3:1206–1216. [PubMed: 2676722]

100. Lardelli RM, Thompson JX, Yates JR, Stevens SW. Release of SF3 from the intron branchpoint activates the first step of pre-mRNA splicing. RNA. 2010; 16:516–528. [PubMed: 20089683]

101. Wlodaver AM, Staley JP. The DExD/H-box ATPase Prp2p destabilizes and proofreads the catalytic RNA core of the spliceosome. RNA. 2014; 20:282–294. [PubMed: 24442613]

102. Liu HL, Cheng SC. The interaction of Prp2 with a defined region of the intron is required for the first splicing reaction. Mol Cell Biol. 2012; 32:5056–5066. [PubMed: 23071087]

103. Chiu YF, Liu YC, Chiang TW, Yeh TC, Tseng CK, Wu NY, Cheng SC. Cwc25 is a novel splicing factor required after Prp2 and Yju2 to facilitate the first catalytic reaction. Mol Cell Biol. 2009; 29:5671–5678. [PubMed: 19704000]

104. Blanco MR, Martin JS, Kahlscheuer ML, Krishnan R, Abelson J, Laederach A, Walter NG. Single Molecule Cluster Analysis dissects splicing pathway conformational dynamics. Nat Meth. 2015; 12:1077–1084.

105. Semlow DR, Blanco MR, Walter NG, Staley JP. Spliceosomal DEAH-Box ATPases remodel pre-mRNA to activate alternative splice sites. Cell. 2016; 164:985–998. [PubMed: 26919433]

106. Ilagan JO, Chalkley RJ, Burlingame AL, Jurica MS. Rearrangements within human spliceosomes captured after exon ligation. RNA. 2013; 19:400–412. [PubMed: 23345524]

107. James SA, Turner W, Schwer B. How Slu7 and Prp18 cooperate in the second step of yeast pre-mRNA splicing. RNA. 2002; 8:1068–1077. [PubMed: 12212850]

108. Aronova A, Bacíková D, Crotti LB, Horowitz DS, Schwer B. Functional interactions between Prp8, Prp18, Slu7, and U5 snRNA during the second step of pre-mRNA splicing. RNA. 2007; 13:1437–1444. [PubMed: 17626844]

109. Maniatis T, Reed R. An extensive network of coupling among gene expression machines. Nature. 2002; 416:499–506. [PubMed: 11932736]

110. Vargas DY, Shah K, Batish M, Levandoski M, Sinha S, Marras SAE, Schedl P, Tyagi S. Single-molecule imaging of transcriptionally coupled and uncoupled splicing. Cell. 2011; 147:1054–1065. [PubMed: 22118462]

111. Coulon A, Ferguson ML, de Turris V, Palangat M, Chow CC, Larson DR. Kinetic competition during the transcription cycle results in stochastic RNA processing. Elife. 2014; 3:e03939.

112. Martin RM, Rino J, Carvalho C, Kirchhausen T, Carmo-Fonseca M. Single-molecule fluorescence-based studies on the dynamics, assembly and catalytic mechanism of the spliceosome. Cell Reports. 2014; 42:1211–1218.

113. Novotný I, Blažíková M, Staněk D, Herman P, Malinsky J. In vivo kinetics of U4/U6.U5 trisnRNP formation in Cajal bodies. Mol Biol Cell. 2010; 22:513–523. [PubMed: 21177826]

114. Staněk D, Pridalová-Hnilicová J, Novotný I, Huranová M, Blazíková M, Wen X, Sapra AK, Neugebauer KM. Spliceosomal small nuclear ribonucleoprotein particles repeatedly cycle through Cajal bodies. Mol Biol Cell. 2008; 19:2534–2543. [PubMed: 18367544]

115. Wan R, Yan C, Bai R, Wang L, Huang M, Wong CC, Shi Y. The 3.8 Å structure of the U4/U6.U5 tri-snRNP: insights into spliceosome assembly and catalysis. Science. 2016; 351:466–475. [PubMed: 26743623]

116. Nguyen THD, Galej WP, Bai XC, Oubridge C, Newman AJ, Scheres SHW, Nagai K. Cryo-EM structure of the yeast U4/U6.U5 tri-snRNP at 3.7 Å resolution. Nature. 2016; 530:298–302. [PubMed: 26829225]

117. Agafonov DE, Kastner B, Dybkov O, Hofele RV, Liu WT, Urlaub H, Lührmann R, Stark H. Molecular architecture of the human U4/U6.U5 tri-snRNP. Science. 2016

118. Mayer A, di Iulio J, Maleri S, Eser U, Vierstra J, Reynolds A, Sandstrom R, Stamatoyannopoulos JA, Churchman LS. Native elongating transcript sequencing reveals human transcriptional activity at nucleotide resolution. Cell. 2015; 161:541–554. [PubMed: 25910208]

119. Nojima T, Gomes T, Grosso ARF, Kimura H, Dye MJ, Dhir S, Carmo-Fonseca M, Proudfoot NJ. Mammalian NET-Seq Reveals Genome-wide Nascent Transcription Coupled to RNA Processing. Cell. 2015; 161:526–540. [PubMed: 25910207]

120. Pandya-Jones A, Black D. Co-transcriptional splicing of constitutive and alternative exons. RNA. 2009; 15:1896–1908. [PubMed: 19656867]

121. Bhatt DM, Pandya-Jones A, Tong AJ, Barozzi I, Lissner MM, Natoli G, Black DL, Smale ST. Transcript Dynamics of Proinflammatory Genes Revealed by Sequence Analysis of Subcellular RNA Fractions. Cell. 2012; 150:279–290. [PubMed: 22817891]

122. Cherny D, Gooding C, Eperon GE, Coelho MB, Bagshaw CR, Smith CWJ, Eperon IC. Stoichiometry of a regulatory splicing complex revealed by single-molecule analyses. EMBO J. 2010; 29:2161–2172. [PubMed: 20502437]

123. Ellis JD, Llères D, Denegri M, Lamond AI, Cáceres JF. Spatial mapping of splicing factor complexes involved in exon and intron definition. J Cell Biol. 2008; 181:921–934. [PubMed: 18559666]

Further Reading

124. Selvin, PR.; Ha, T. A Laboratory Manual. New York: Cold Spring Harbor Laboratory Press; 2008. Techniques.

125. Hertel, KJ. Spliceosomal Pre-mRNA Splicing. In: Walker, JM., editor. Methods in Molecular Biology. Vol. 1126. New York: Humana Press; 2008.

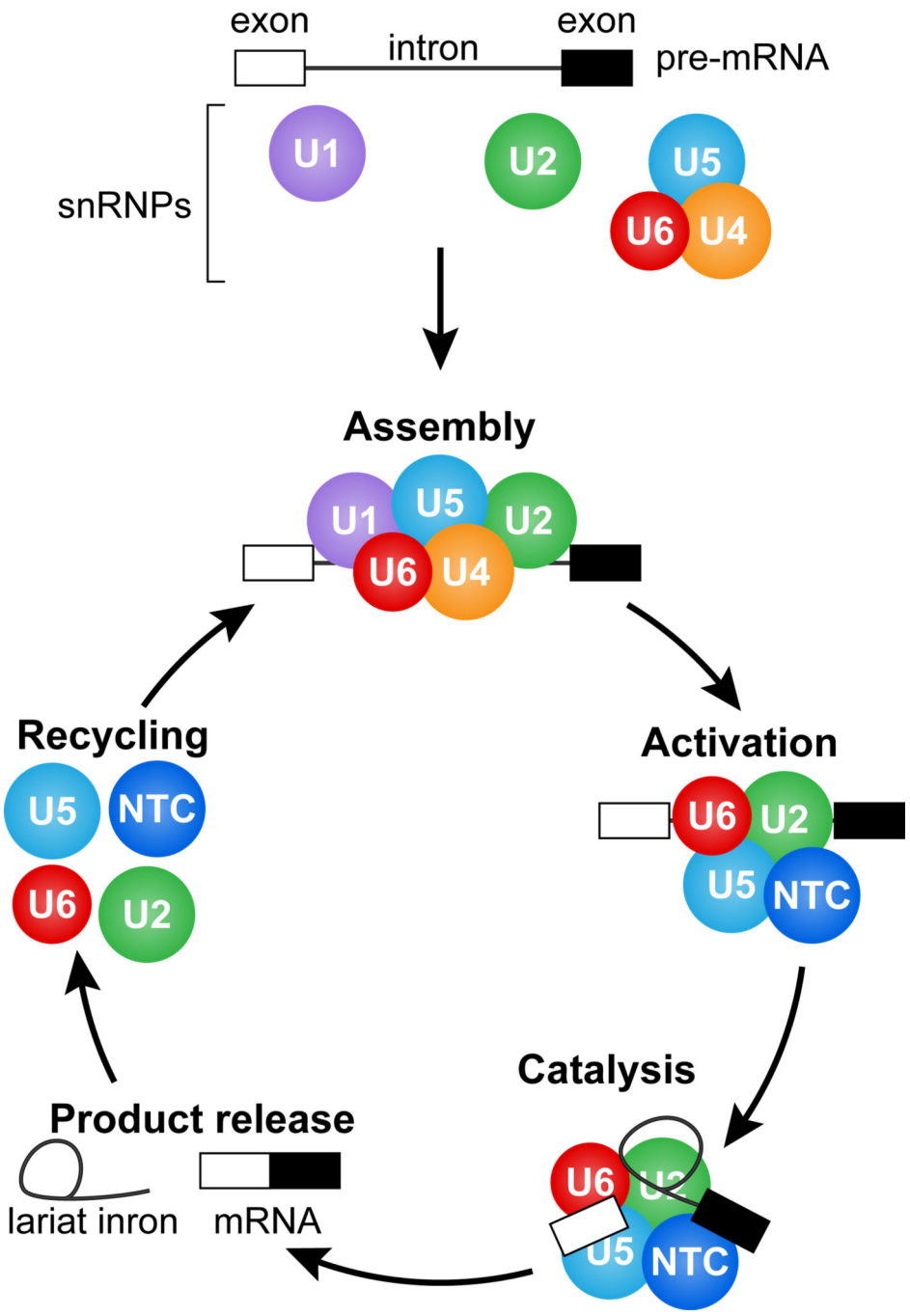

Figure 1. Schematic Overview of the Major Stages in Splicing

Splicing occurs through distinct stages of assembly, activation, catalysis, product release, and recycling of the splicing machinery. During assembly, the snRNPs (U1, U2, and the U4/U6.U5 tri-snRNP) assemble on a pre-mRNA substrate to form the spliceosomal B complex. During activation, U1 and U4 are expelled, and the Prp19-associated complex (NTC) joins the spliceosome. After action of the ATPase Prp2, the first chemical step of splicing occurs, and the spliceosomal C complex is formed. After exon ligation, mRNA and lariat intron

products are released from the spliceosome and the splicing machinery is recycled to begin a new round of splicing on another intron.

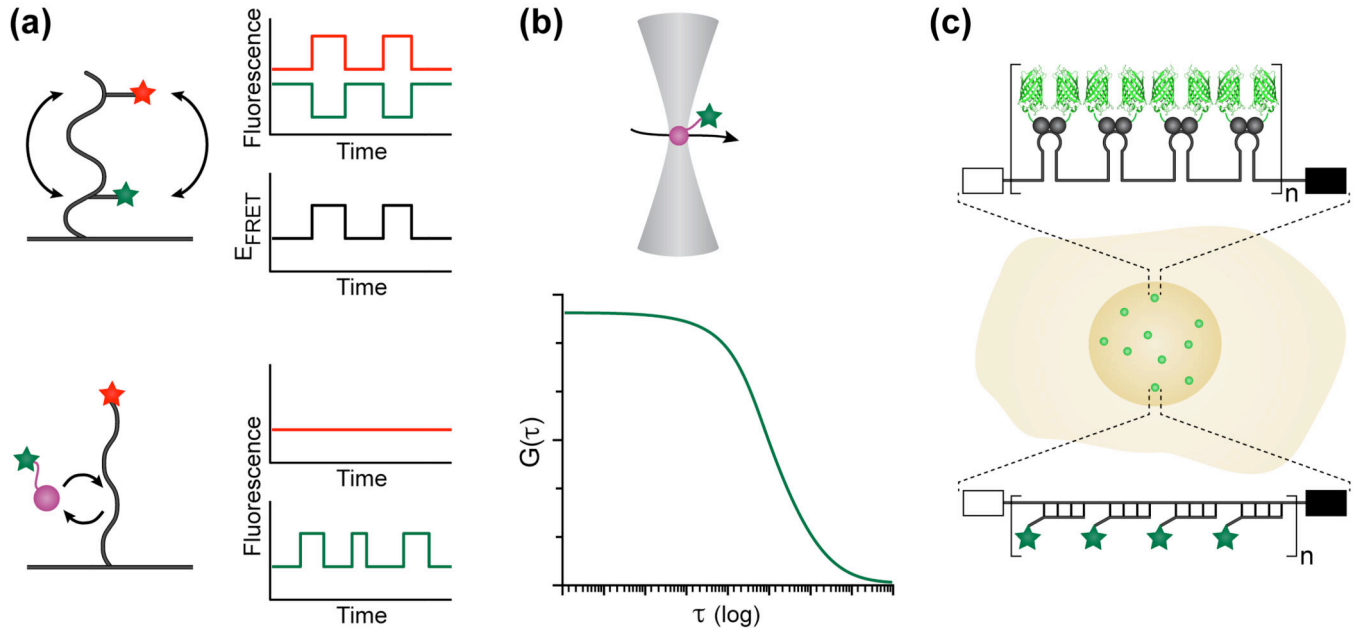

Figure 2. Overview of Single Molecule Fluorescence Techniques

(a) Illustration of simple, tethered molecule smFRET (top) and colocalization (bottom) single molecule fluorescence experiments. In smFRET, donor (green trace and star) and acceptor (red trace and star) fluorescence intensities are anti-correlated and can be used to calculate E_{FRET}. In colocalization experiments, peaks of fluorescence intensity (green) represent binding events occurring between a freely diffusing molecule and a tethered substrate. (b) Illustration of a single molecule experiment carried out with a freely diffusing fluorescent molecule and using confocal microscopy. As the molecule passes through the confocal volume (shown), fluorescence can be detected. Many individual events can be studied using correlation analysis to produce a plot of correlation [G(**τ**)] vs. a given time constant. The shape of the correlation curve is indicative of the diffusive properties of the molecule as well as molecular concentration. (c) In cells, single RNA transcripts can be imaged by targeting many fluorophores (n = dozens or hundreds of fluorescent molecules) to the RNA. In live cells this can be accomplished by encoding a binding site for an RNA binding protein-FP fusion (top). In fixed cells, transcripts can be detected by hybridization of complementary, fluorescent oligos.

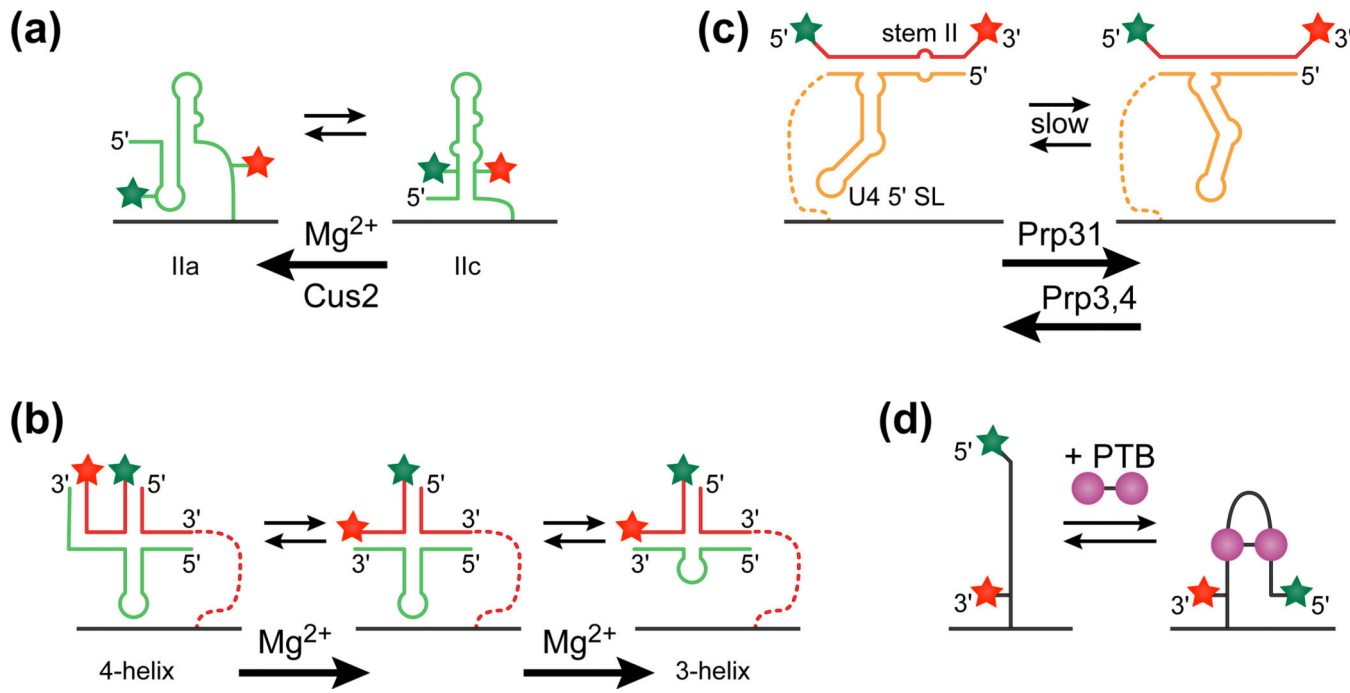

Figure 3. Insights into RNA Dynamics from smFRET of Model Systems

(a) Using a model for the U2 snRNA stem II region (green), Rodgers *et al.* were able to show that the RNA toggles spontaneously between IIc and IIa conformations. Addition of Mg^{2+} or Cus2 protein strongly promoted accumulation of IIa conformers. (b) By employing a model for the U2 (green)/U6(red) di-snRNA, Guo *et al.* revealed Mg^{2+} dynamics that may correspond to switching of the RNA model between 3-helix and 4-helix structures. (c) Hardin *et al.* used a model for the U4 (orange)/U6(red) di-snRNA to show that, despite few intrinsic dynamics, addition of U4/U6 di-snRNP proteins (Prp3, 4, and 31) were able to change the relative orientation of the U4 5' stem loop (SL) and U4/U6 stem II. (d) Lamichhane *et al.* developed a smFRET-based RNA looping assay to study the interaction of a fragment of PTB with labeled RNAs.

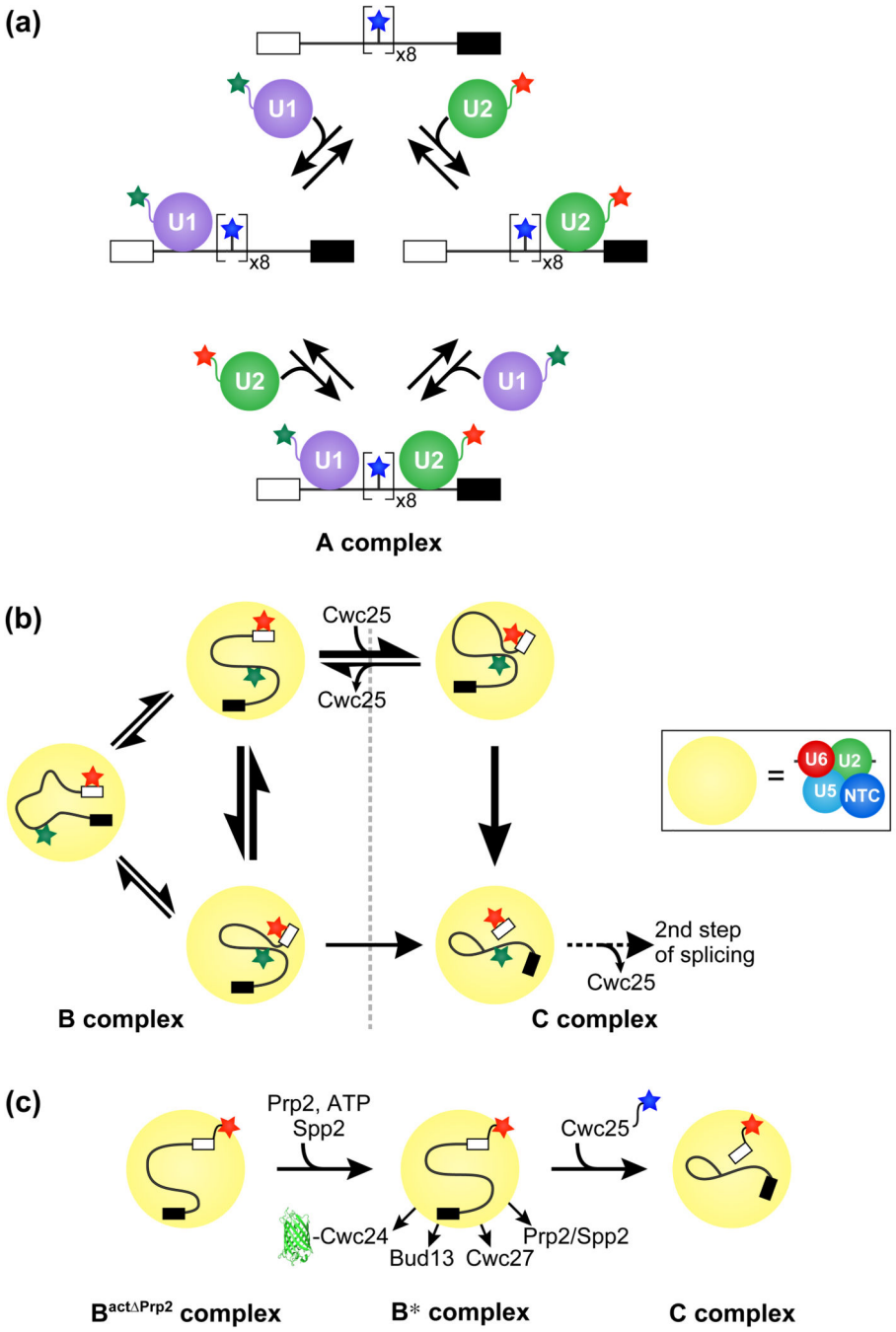

Figure 4. Insights into Spliceosomes from Single Molecule Fluorescence

(a) Using a combination of labeled snRNPs, pre-mRNA substrates, and CoSMoS, Shcherbakova *et al.* were able to show that functional yeast spliceosomes can assemble via either U1-first or U2-first pathways. (b) smFRET experiments from Krishnan and coworkers revealed pre-mRNA dynamics that persist after activation of the spliceosome by Prp2. Cwc25 is hypothesized to bias the conformational dynamics of the spliceosome towards a structure in which the 5' SS and BS are proximal, thus promoting the first chemical step in splicing. (c) By making use of purified spliceosomes and dcFCCS, Ohrt et al. were able to

study the binding properties of a number of splicing factors as the spliceosome progressed through activation and the chemical steps of splicing. In some cases, Ohrt et al. were able to use dcFCCS to study the dynamics of GFP labeled proteins (*e.g.*, Cwc24) while in other cases the proteins were labeled with organic fluorophores (*e.g.*, Cwc25). Prp2 activity destabilizes a number of splicing factors while promoting Cwc25 association, which in turn facilitates 5' SS cleavage. Figures have been adapted from models described in references 85, 86, and 89.

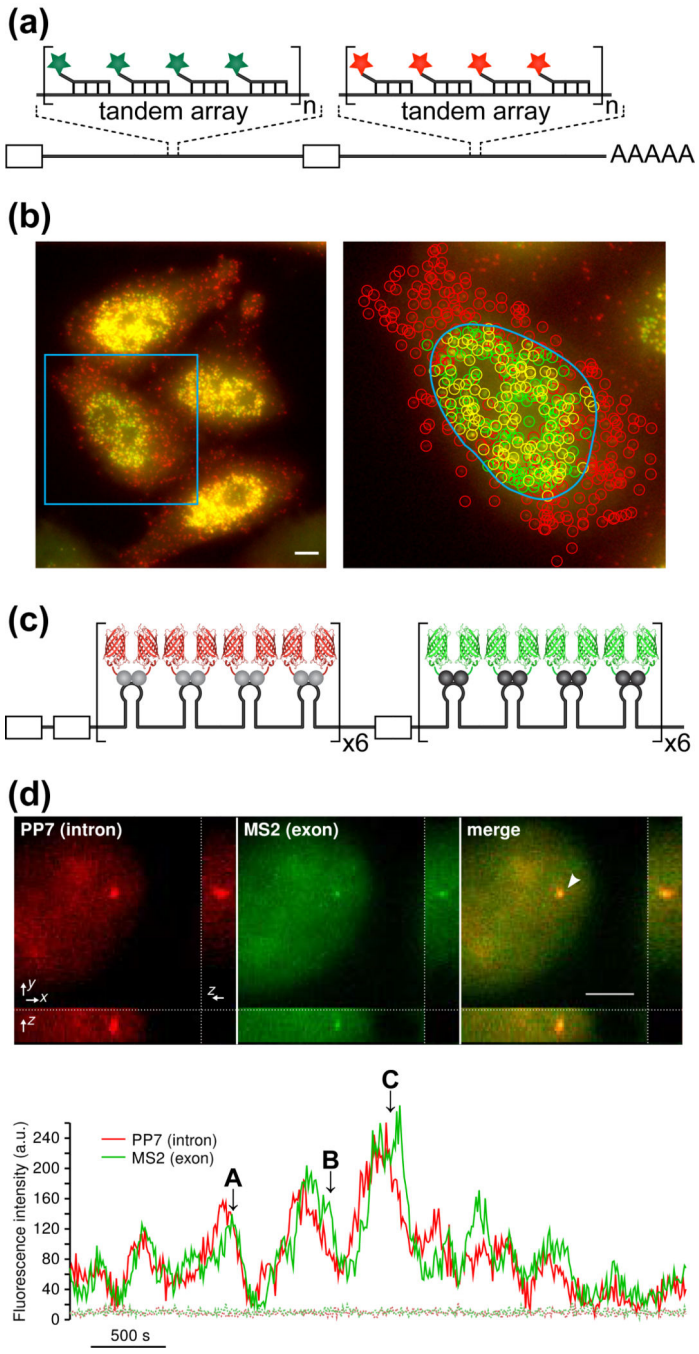

Figure 5. Studies of Splicing in Fixed and Live Cells

(a) Schematic of the smFISH-based strategy developed by Vargas *et al.* to study co-transcriptional splicing in fixed cells. Reporter RNAs were labeled by insertion of repetitive sequences that can be targeted by multiple fluorescent, complementary oligos. (b) Microscopic images (left) and colocalization data (right) obtained by Vargas *et al.* using the approach described in (a). Bright spots correspond to single transcripts bound to the fluorescent probes. Red circles in the colocalization data denote mRNA locations, green circles represent processed introns, and yellow circles represent unspliced pre-mRNAs or

spliceosome-bound mRNA/intron complexes. The nuclear boundary is shown with a blue, dashed line. (c) Schematic of the RNA binding protein-based strategy developed by Coulon *et al.* to study co-transcriptional splicing in live cells. Reporter RNAs were labeled by insertion of MS2 or PP7 stemloops that can be targeted by PP7-mCherry or MS2-GFP fusion proteins. (d) Microscopic images (top) and fluorescence time trajectories (bottom) obtained by Coulon and coworkers using the approach described in (c). In the microscopic images (top) a pre-mRNA or spliceosomal complex containing both an intron and 3' UTR signal is identified by colocalization of the green and red spots of fluorescence (arrow head). In the fluorescence trajectories (bottom) multiple rounds of transcription and splicing can be observed (peaks). In some cases (peaks B and C), the red, intronic signal disappeared before the green 3' UTR signal, consistent with co-transcriptional splicing. In other cases (peak A), both signals disappeared simultaneously consistent with the completion of splicing after the end of transcription. Data in (b) and (d) were obtained from references 110 and 111, respectively, and are used with permission.

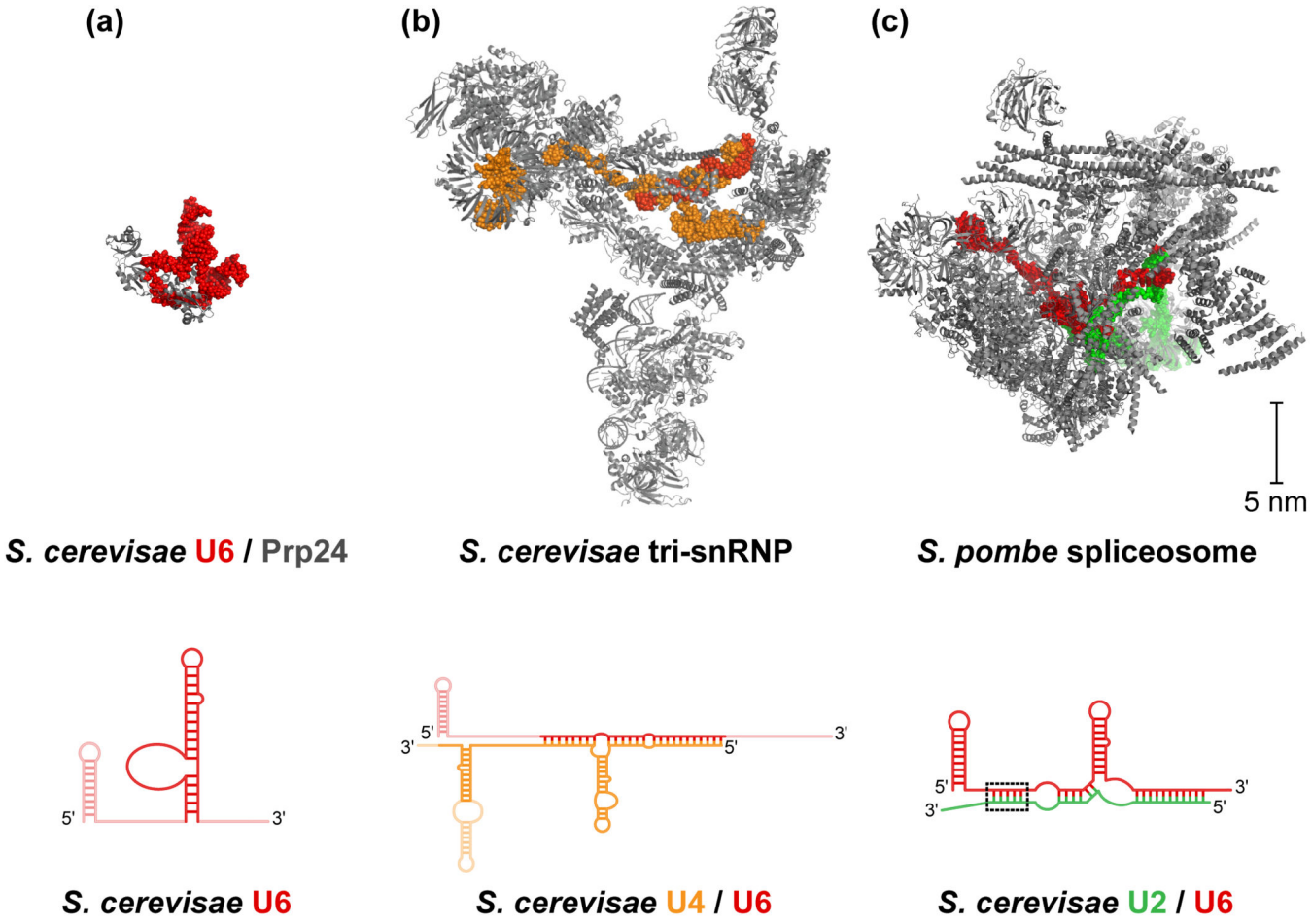

Figure 6. Structural Insights into U6 snRNA Conformational Changes during Splicing

(a, top) Structure of a portion of the yeast U6 snRNA (red) bound to yeast Prp24 (grey). (a, bottom) Proposed basepairing structure of the yeast U6 snRNA. Darker regions are those observed in the U6/Prp24 crystal structure, lighter regions were either not observed or crystallized. (b, top) Cryo-EM structure of the yeast tri-snRNP highlighting the U6 (red) and U4 (orange) snRNAs. (b, bottom) Proposed basepairing structure of the yeast U4/U6 di-snRNA. Darker regions are those modeled in the cryo-EM structure at top, lighter regions were either not observed or modeled. (c, top) Cryo-EM structure of the *S. pombe* U2/U6.U5 spliceosomal complex highlighting the U6 (red) and U2 (green) snRNAs. (c, bottom) Proposed basepairing structure of the *S. cerevisiae* U2/U6 snRNA. The boxed region represents helix III, which was not observed in the *S. pombe* spliceosome structure. Structures in (a)-(c) are all shown to scale. Figures for (a) and (c) were prepared from 4NOT.pdb and 3JB9.pdb, respectively. Coordinates for the tri-snRNP model in (b) were generously provided by K. Nagai (MRC, Cambridge, UK).